Life Sciences 219 (2019) 248–256

Contents lists available at ScienceDirect

Life Sciences

journal homepage: www.elsevier.com/locate/lifescie

PIM inhibitor SMI-4a induces cell apoptosis in B-cell acute lymphocytic leukemia cells via the HO-1-mediated JAK2/STAT3 pathway

Xingyi Kuang[a,b,c], Jie Xiong[a,b,c], Weili Wang[a,b,c], Xinyao Li[a,b,c], Tingting Lu[a,b,c], Qin Fang[d], Jishi Wang[a,b,c,*]

[a] Department of Hematology, The Affiliated Hospital of Guizhou Medical University, Guiyang, PR China
[b] Guizhou Province Hematopoietic Stem Cell Transplantation Center, The Affiliated Hospital of Guizhou Medical University, Guiyang, PR China
[c] Key Laboratory of Hematological Disease Diagnostic Treat Centre of Guizhou Province, Guiyang, PR China
[d] Department of Pharmacy, The Affiliated Baiyun Hospital of Guizhou Medical University, Guiyang, Guizhou, PR China

ARTICLE INFO

Keywords:
B-ALL
SMI-4a
JAK2/STAT3
Apoptosis

ABSTRACT

Objectives: The serine/threonine PIM protein kinases are critical regulators of tumorigenesis in multiple cancers. However, whether PIMs are potential therapeutic targets for treating B-cell acute lymphocytic leukemia (B-ALL) remains unclear. Therefore, here, PIM expression was detected in B-ALL patients and the effects of SMI-4a, a pan-PIM small molecule inhibitor, were investigated in B-ALL cells.

Methods: PIM1 and PIM2 expression in 26 newly diagnosed B-ALL cases was detected by real-time PCR and Western blot. B-ALL cells were treated with varied SMI-4a doses and the viability of treated cells was investigated using a cell-counting kit-8 (CCK-8) assay. Apoptosis and cell cycles were analyzed by flow cytometry. Western blot analysis was then used to explore the expression of apoptosis-related proteins and the JAK2/STAT3 pathway.

Results: PIM1 and 2 were overexpressed in B-ALL patients with high HO-1 level. SMI-4a induced decreases in PIMs and HO-1 expressions and inhibited B-ALL cell viability. Treatment with SMI-4a induced apoptosis by downregulating Bcl-2, upregulating Bax and other antiapoptotic proteins, and decreasing protein levels of p-JAK2 and p-STAT3. In addition, upregulation of HO-1 alleviated decrease in p-JAK2 and p-STAT3 expression, reduced SMI-4a-induced apoptosis of B-ALL cells, and influenced B-ALL cell survival.

Conclusions: PIMs were highly expressed in B-ALL patients. SMI-4a inhibited B-ALL proliferation and induced apoptosis via the HO-1-mediated JAK2/STAT3 pathway. SMI-4a might be applicable for treatment of B-ALL cells.

1. Introduction

B-cell acute lymphoblastic leukemia (B-ALL), a blood cancer derived from immature B-cell precursors, usually affects children under 6 years of age but also occurs in older children and adults. The global incidence of B-ALL is estimated at approximately 1–5 per 100,000 people per year. Patients with B-ALL usually have symptoms and signs of bone marrow (BM) failure, including cytopenia with or without leukocytosis [1]. Despite a better understanding of the disease biology and the use of multidrug chemotherapy, the long-term survival rate of B-ALL adults varies from 35 to 50% [2]. As the treatment of patients with refractory/recurrent B-ALL remains a clinical challenge, it is thus very important to explore new therapeutic strategies for clinical treatment of this disease.

The serine/threonine PIM protein kinases are critical regulators of tumorigenesis in multiple hematologic malignancies and solid cancers [3–6]. There are three serine/threonine protein kinases members of the PIM kinases, including PIM-1, 2, and 3, which are involved in regulation of survival, apoptosis, cell cycle, and drug resistance [4,7,8]. Recent studies have shown that serine/threonine PIM protein kinases are overexpressed in multiple hematopoietic tumors, including acute myeloid leukemia (AML) [9], multiple myeloma (MM) [10], chronic lymphocytic leukemia [6], and non-Hodgkin lymphoma [11]. In addition, High PIM protein kinase expression predicates poor prognoses in various cancers [3,12]. More importantly, PIM protein kinase genes are critical oncogenes in various hematologic malignancies and solid cancers. In pancreatic cancer cells, PIM-1 knockdown suppressed proliferation, induced cell-cycle arrest, and enhanced apoptosis [3]. Targeting PIM-1 with small inhibitors in T-cell leukemia and lymphoma

* Corresponding author at: Department of Hematology, Affiliated Hospital of Guizhou Medical University, Guiyang, Guizhou 550004, PR China.
E-mail address: wangjishi9646@163.com (J. Wang).

https://doi.org/10.1016/j.lfs.2019.01.022
Received 11 September 2018; Received in revised form 3 January 2019; Accepted 14 January 2019
Available online 16 January 2019
0024-3205/ © 2019 Published by Elsevier Inc.

(ATL) cells induces apoptosis and reduces tumor growth in a xenograft mouse model of ATL [13]. In MM cells, PIM-2 silencing by siRNA clearly inhibits growth of MM cell lines through the JAK2/STAT3 pathway [4]. Similarly, PIM-2 knockdown reduces Burkitt lymphoma cell growth [14]. Taken together, these results support an oncogenic role for PIM protein kinase.

SMI-4a is a pan-PIM small molecule inhibitor, which exhibits demonstrable preclinical antitumor activity in a wide range of hematologic malignant cell lines, including human and murine precursor T-cell lymphoblastic leukemia/lymphoma (pre-T-LBL) cells [15], non-Hodgkin lymphomas [11], and chronic myeloid leukemia cells (CML) [16]. Also, emerging evidence has revealed a function of SMI-4a in regulating cell cycle and apoptosis [15,16]. However, the exact role of PIM kinase inhibitor as a therapeutic target in B-ALL remains unclear. In the current study, PIM expression was investigated in B-ALL patients. The effects of SMI-4a on cell growth, apoptosis, and cell cycle were assessed in B-ALL-derived cell lines. Finally, the mechanisms that mediated the effects of this small molecule on B-ALL cells were examined in detail.

2. Materials and methods

2.1. Reagents and antibodies

Non-selective PIM inhibitor SMI-4a was purchased from MedChemExpression (New Jersey, USA). HO-1 inhibitor ZnPP was purchased from Cayman Chemical (Ann Arbor, MI, USA). Hemin was obtained from Sigma (St. Louis, MO, USA). Antibodies specific for PIM-1, PIM-2, β-actin, STAT3, Bcl-2, Bax and HO-1 were purchased from MDL biotech (Beijing, China). Polyclonal primary antibodies against Caspase-3, Caspase-8, Caspase-9, P21, Cyclin D1, CDK4, p-STAT3, JAK2 and p-JAK2 were bought from Santa Cruz (Heidelberg, Germany). Secondary antibodies (HRP-conjugated goat anti-rabbit or anti-mouse) were purchased from Beyotime (Shanghai, China).

2.2. Patients and specimens

For PIM expression analysis, bone marrow samples were obtained from 26 newly diagnosed B-ALL patients in The Affiliated Hospital of Guizhou Medical University (Table 1). Mononuclear cells were separated from bone marrow by Ficoll gradient centrifugation. The diagnosis of B-ALL were established according to 2016 WHO criteria. This study was approved by the institutional review board of The Affiliated Hospital of Guizhou Medical University and all patients offered informed consent according to the Declaration of Helsinki.

Table 1
Patients' characteristics.

	Descriptive statistics
Total patients	26
Median age, years (minimum–maximum)	21 (1–48)
Age	
< 10	6 (23.1%)
10–40	16 (61.5%)
> 40	4 (15.4%)
White blood cells count ($\times 10^9$/L)	
< 10	16 (61.5%)
10–99	5 (19.2%)
≥100	5 (19.2%)
Cytogenetics	
Ph (+)	8 (30.8%)
TEL-AML1 (+)	2 (7.7%)
Normal	16 (61.5%)
Immunophenotype	
Pro-B-ALL	2 (7.7%)
Pre-B-ALL	3 (11.5%)
Common-B-ALL	21 (80.8%)

2.3. Cell culture

Human B-ALL cell lines CCRF-SB and Sup-B15 were obtained from Guizhou Province Laboratory of Haematopoietic Stem Cell Transplantation Center. The cell lines were cultured in RPMI-1640 medium (Gibco, Carlsbad, CA, USA) supplemented with 10% fetal bovine serum (Tianhang Biotechnology, Zhejiang, China) and 1% penicillin/streptomycin (Invitrogen, Carlsbad, USA) at 37 °C/5% CO_2.

2.4. Cell counting kit-8 (CCK-8) proliferation assay

Cell proliferation was evaluated using a CCK-8 assay after SMI-4a treatment. B-ALL cells were seeded into 96-well plates at a density of 5×10^3 cells/well with 3 replicate wells of each condition. For the CCK-8 assay, 10 μL of CCK-8 solution (Dojindo, Kumamoto, Japan) was added to each well and incubated at 37 °C for 2 h. Absorbance values at 450 nm were measured using spectrophotometer (Molecular Devices, Sunnyvale, California, USA).

2.5. Annexin V-FITC/propidium iodide (PI) staining for apoptosis analysis

After incubation with SMI-4a in serum-free medium, B-ALL cells were harvested and washed with cold phosphate-buffered saline (PBS), then stained with 3.5 μL of AnnexinV-FITC (KeyGen Biotech, Shanghai, China) and 5 μL of PI (KeyGen Biotech) in dark. After that, the number of apoptotic cells were measured by flow cytometry using Cell Quest software (BD Biosciences, San Jose, CA, USA).

2.6. Cell cycle analysis

Cells were harvested, washed once in ice-cold PBS, fixed in 70% ethanol at 4 °C for > 2 h, then incubated in staining cocktail containing 50 μg/mL PI (7Sea Biotech, Shanghai, China) and 50 μg/mL RNase (7Sea Biotech) for 30 min at 37 °C in dark. DNA content of samples were analyzed with the use of FACSCalibur flow cytometer (BD Biosciences) and Multicycle software.

2.7. Quantitative reverse transcriptase-polymerase chain reaction (qRT-PCR)

Total RNA was extracted from cells using Trizol reagent (Invitrogen), reversely transcribed with the use of Revertaid First Strand cDNA Synthesis Kit (Thermo Scientific, Waltham, Massachusetts, USA). Each reverse transcription reaction was performed in 20 μL reaction volume containing 0.1 μg of total RNAs, 1 μL Random Hexamer primer, 4 μL of 5 × Reaction Buffer, 1 μL RiboLock RNase Inhibitor, 2 μL of 10 mM dNTP Mix, and 1 μL RevertAid M-MuLV RT. Reverse transcription conditions were as follows: 25 °C for 5 min, 42 °C for 60 min, and 70 °C for 5 min. The reverse transcription products were amplified using a SYBR Green PCR Master Mix (TianGen Biotech, Beijing, China) on the ABI 7500 real-time PCR detection system for 10 min at 95 °C, followed by 40 cycles at 95 °C for 15 s and at 60 °C for 1 min. For mRNA quantification, β-actin was selected as the internal control. Real-time PCR specific primers were shown as follows: PIM-1 F: 5′-GTGGAGGTGGATCTCAGCAGT-3′, PIM-1 R: 5′-GTTTTCTTCAGGCAGAGGGTC-3′; PIM-2 F: 5′-TACATCCTCGGCTGGTCTTTG-3′, PIM-2 R: 5′-ACTGTCTGGTCACTGGGCATC-3′; PIM-3 F: 5′-GTCCACAAGCAGATTTTCGTC-3′, PIM-3 R: 5′-CAGGACCTCTTCGACTTTATCA-3′; HO-1, F: 5′-ACCCATGACACCAAGGACCAGA-3′; HO-1, R: 5′-GTGTAAGGACCCATCGGAGAAGC-3′; β-actin F: 5′-GACATCCGCAAAGACCTG-3′, β-actin R: 5′-GGAAGGTGGACAGCGAG-3′.

2.8. Western blot analysis

Protein lysate was extracted from cells using RIPA lysis buffer supplemented with 1 μM PMSF (Solarbio Science & Technology,

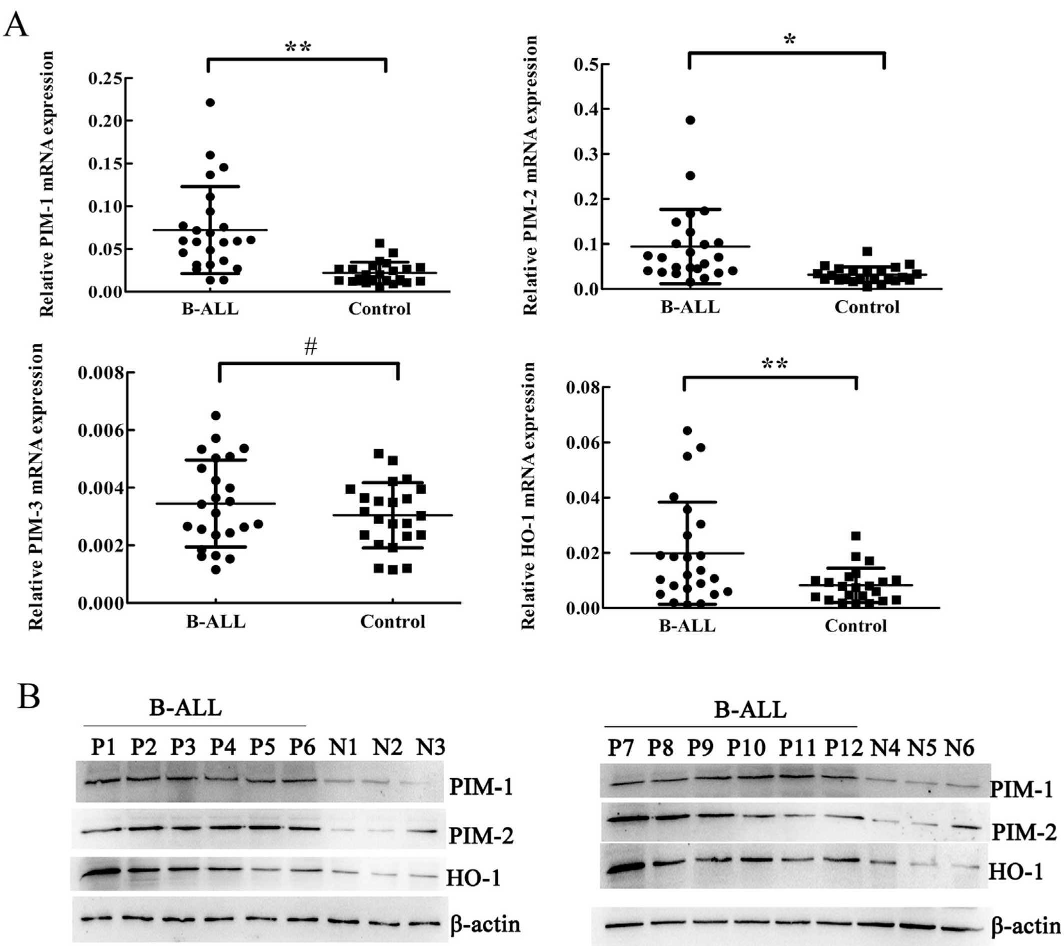

Fig. 1. Expression levels of PIMs and HO-1 in B-ALL patients. (A) The mRNA expression of PIM-1, 2, and 3 and HO-1 in BM-MNCs of B-ALL patients (n = 26) detected by real-time PCR. Data represented as mean ± SD; *, $p < 0.05$ compared with healthy controls; **, $p < 0.01$ compared with healthy controls; and $^{\#}$, $p > 0.05$ compared with healthy controls. (B) PIM-1, PIM-2 and HO-1 protein levels in B-ALL patients determined by Western blot. Loading control, β-actin.

Beijing, China) agitated at 4 °C for 30 min followed by centrifugation for 10 min. Supernatants were then loaded on 10% SDS–PAGE gel and the separated proteins transferred onto PVDF membranes. Membranes were routinely blocked in 5% nonfat milk in PBS for 2 h with agitation and washed. Then, the membrane was blotted with primary antibodies for 2 h. After washing, the membranes was incubated with secondary antibodies (HRP-conjugated goat anti-rabbit or anti-mouse; Beyotime) for 45 min at room temperature. All protein bands were visualized with the use of the enhanced chemiluminescence (7Sea Biotech).

2.9. In vivo study

Female 5 to 6-week-old Non-obese diabetic severely compromised immunodeficient (NOD/SCID) mice were obtained from Beijing HEK Bioscience. CCRF-SB cells (1×10^7) were implanted with matrigel (BD Biosciences) subcutaneously into the left flank of mice. All mice were randomly assigned to vehicle only (DMSO + Saline) or 60 mg/kg SMI-4a twice daily treatment [15]. Tumor volume was measured twice per week with calipers and calculated as tumor volume (mm^3) = L × W^2/2 (L represents the largest diameter; W is the smallest diameter of tumor). All animal experiments were approved by the Ethics Committee of GuiZhou Medical University.

2.10. Histological analysis

The xenograft tumors were fixed in 4% paraformaldehyde solution, embedded in paraffin and cut into 3 μm-thick sections. Then the paraffin sections were stained with hematoxylin and eosin (H&E). DNA fragmentation in nucleus, which is a typical feature of apoptosis, can be detected by the terminal dUTP nick endlabeling (TUNEL) assay. We employed TUNEL assay to evaluate the cell apoptosis in situ using a TUNEL apoptosis assay kit (Beyotime) according to producer's manual. Cell counting was conducted on four random fields of each section [17], and cells with dark brown nuclei were identified as apoptotic cells. Final data were expressed as the percentages of apoptotic cells.

2.11. Statistical analysis

All statistical analyses were performed with SPSS software 20.0. Results were presented as mean ± standard deviation (SD). Two-tailed Student's *t*-test was carried out to determine significance when only two groups were compared. Variations between groups were analyzed with one-way ANOVA, followed by Tukey multiple comparison test. $p < 0.05$ was considered statistically significant.

3. Results

3.1. Expression levels of PIMs and HO-1 in B-ALL patients

PIM kinases are widely expressed in cancer, with higher expression in hematologic than solid malignancies [10]. There are three members of PIM protein kinases including PIM-1, PIM-2 and PIM-3. PIM-3, although expressed in the whole blood system of a malignant tumor, does not show a distinct expression pattern. In particular, PIM-3 has the least

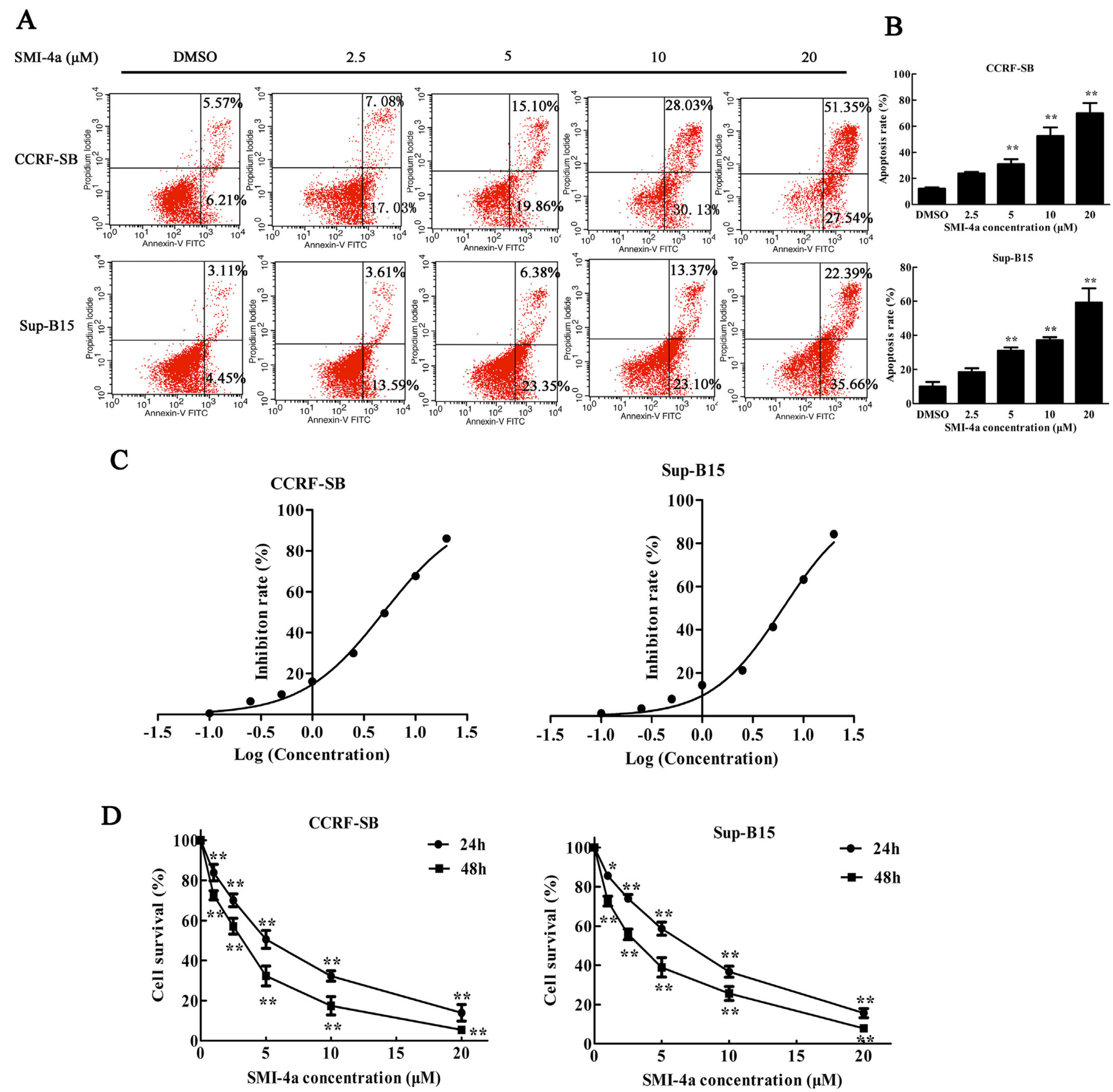

Fig. 2. SMI-4a suppressed B-ALL cell growth and induced B-ALL cell apoptosis. (A) Apoptotic rates of CCRF-SB and Sup-B15 assessed by Annexin V-FITC/PI staining after treatment with 0, 2.5, 5, 10, and 20 μM SMI-4a for 24 h. Data shown for three independent experiments. (B) Analysis of apoptotic rates of CCRF-SB and Sup-B15 cells in three independent experiments. Data presented as mean ± SD; *, $p < 0.05$ versus DMSO group, and **, $p < 0.01$ versus DMSO group. (C) Cells were treated with SMI-4a at 0–20 μM for 24 h examined by CCK-8 assay. The OD_{450} measured and IC_{50} value obtained using Graphpad software 5. (D) Sup-B15 and CCRF-SB cells treated with 0, 1, 2.5, 5, 10, and 20 μM SMI-4a for 24 and 48 h, respectively, and viability detected by CCK-8 assay. Data presented as mean ± SD; *, $p < 0.05$ versus 0 μM group; and **, $p < 0.01$ versus 0 μM group.

correlation with hematological malignancies and is closely related to solid organ malignancies [18]. Hence, the expression of PIM-1, 2, and 3 were first determined in bone marrow mononuclear cells (BM-MNCs) of B-ALL patients and healthy controls using real-time PCR (Fig. 1A). Consistently, B-ALL patients showed significantly higher PIM-1 and 2 mRNA expressions than healthy controls ($p = 0.002$ and 0.015, respectively), while PIM-3 showed no significant difference between B-ALL patients and healthy donors ($p = 0.356$). In addition, HO-1 mRNA level was clearly elevated in B-ALL patients ($p = 0.007$). Western blot analyses also revealed higher expression levels of PIM-1 and 2 proteins in B-ALL patients (Fig. 1B).

3.2. SMI-4a inhibited B-ALL cell growth in vitro

Although there have been many studies showing that PIM kinase inhibitor SMI-4a blocks the growth of various leukemic cells, no study to date has investigated the effects of SMI-4a on B-ALL cell lines. To explore for a strategy for clinical treatment, B-ALL cell lines Sup-B15 and CCRF-SB were treated with different SMI-4a concentrations for 24 and 48 h and the resulting cell viability tested by CCK-8 assay. After

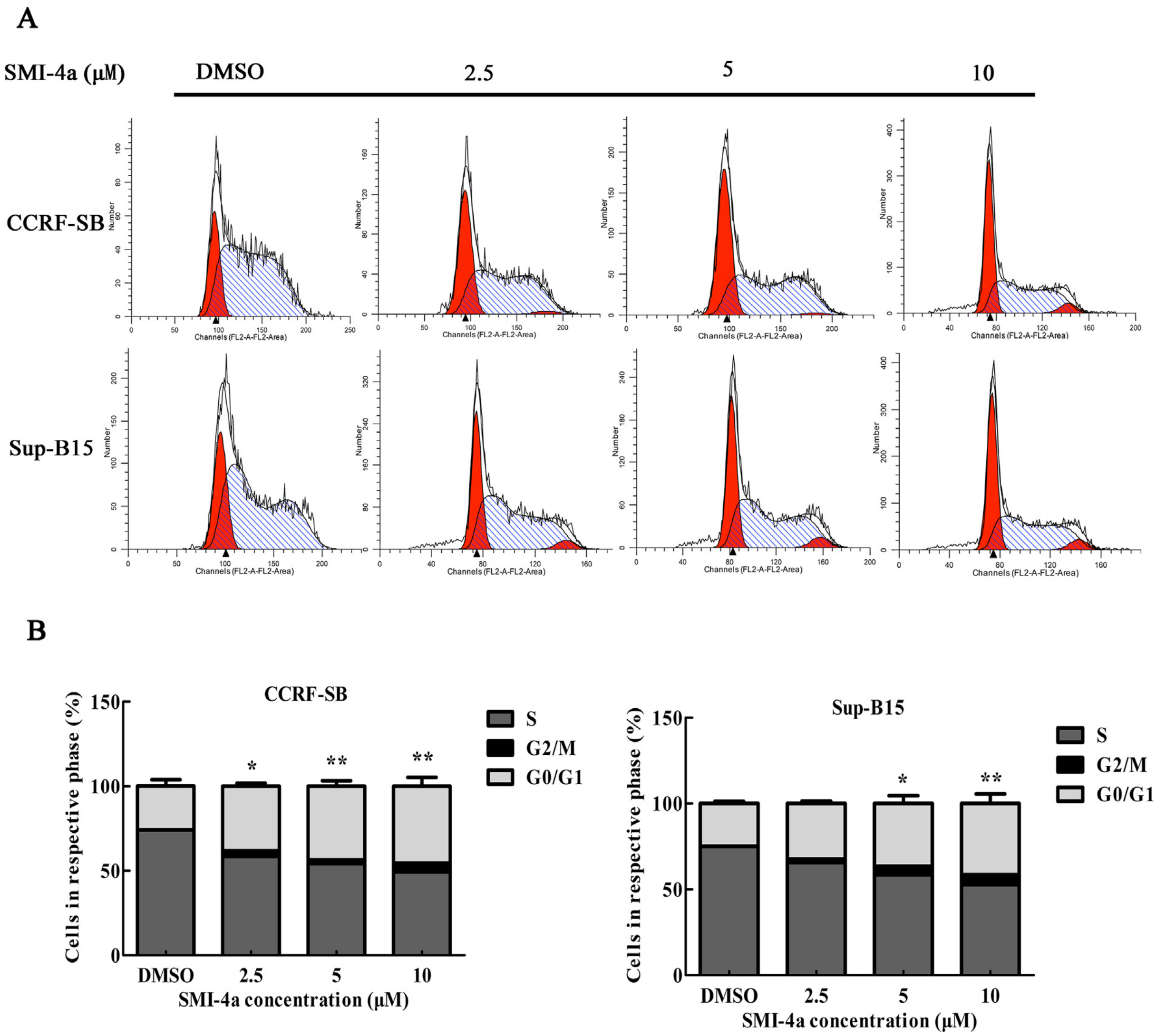

Fig. 3. SMI-4a caused accumulation of B-ALL cells in the G_0/G_1 phase. (A) Sup-B15 and CCRF-SB cells treated with 0, 2.5, 5, and 10 μM SMI-4a for 24 h and then stained with PI and subjected to flow cytometric analysis. Data shown are representative images depicting cell cycle distribution of B-ALL cells. (B) Proportion of cells in various phases of cell cycle. Data presented as mean ± SD; *, $p < 0.05$ versus DMSO group; and **, $p < 0.01$ versus DMSO group.

treatment with SMI-4a, cell survival was significantly inhibited in two B-ALL cell lines (CCRF-SB and Sup-B15) in a dose and time-dependent manner. These data demonstrated that CCRF-SB cells were more sensitive to SMI-4a than Sup-B15 cells (IC_{50} = 4.914 and 6.273, respectively) (Fig. 2C). In addition, cell viabilities of Sup-B15 and CCRF-SB treated by SMI-4a for 48 h were higher than after SMI-4a treatment for 24 h (Fig. 2D).

3.3. Effects of SMI-4a on apoptosis and cell cycle in B-ALL cells

The mechanism by which SMI-4a inhibited B-ALL cell proliferation was investigated by first exploring the ability of this agent to regulate cell apoptosis in B-ALL cells incubated with various doses of SMI-4a. Treatment with SMI-4a increased the apoptotic cell population in a concentration-dependent manner (Fig. 2A). After treatment with 5 μM SMI-4a, the apoptotic rate of Sup-B15 was 29.73% but that of CCRF-SB cells increased to 34.96% (Fig. 2B). In addition, after SMI-4a treatment, the observed Bcl-2 protein expression decreased and Bax increased. SMI-4a also induced upregulation of Caspase-3 and 9, whereas Caspase-8 protein was not altered, which indicated that SMI-4a induced apoptosis via an intrinsic apoptosis pathway. With increased time, apoptosis proteins increased and Bax protein increased early, at 6 h (Fig. 4A and C).

It is well known that changes in cell cycle progression are one of the reasons for cell apoptosis. Some reports have described that down-regulated PIMs not only induce G_1/S and S phase arrest but also led to cell apoptosis [16,19]. Whether SMI-4a had an effect on the cell cycle of B-ALL cells was investigated next and the results of flow cytometry indicated that cells were blocked in G_0/G_1 phases by SMI-4a (Fig. 3A). After treatment with 10 μM SMI-4a, the cell population increased in the G_1 phase from 25.93 to 45.62% and from 24.86 to 41.38% in CCRF-SB and Sup-B15, respectively, whereas the percentage of cells in S phase decreased in both cell lines (Fig. 3B). In addition, the expressions of several proteins related to G_1/S cell cycle progression were detected by Western blot, which showed that CDK4 and Cyclin D1 decreased, while P21 increased (Fig. 4B).

3.4. SMI-4a induced apoptosis partly through an HO-1-mediated JAK2/STAT3 pathway

A previous study has shown that SMI-4a modulates the JAK2/STAT3 pathway in Reed-Sternberg cells [14], that constitutive STAT activation is present in many malignancies, and has been especially well characterized in acute and chronic leukemias [20]. To examine whether

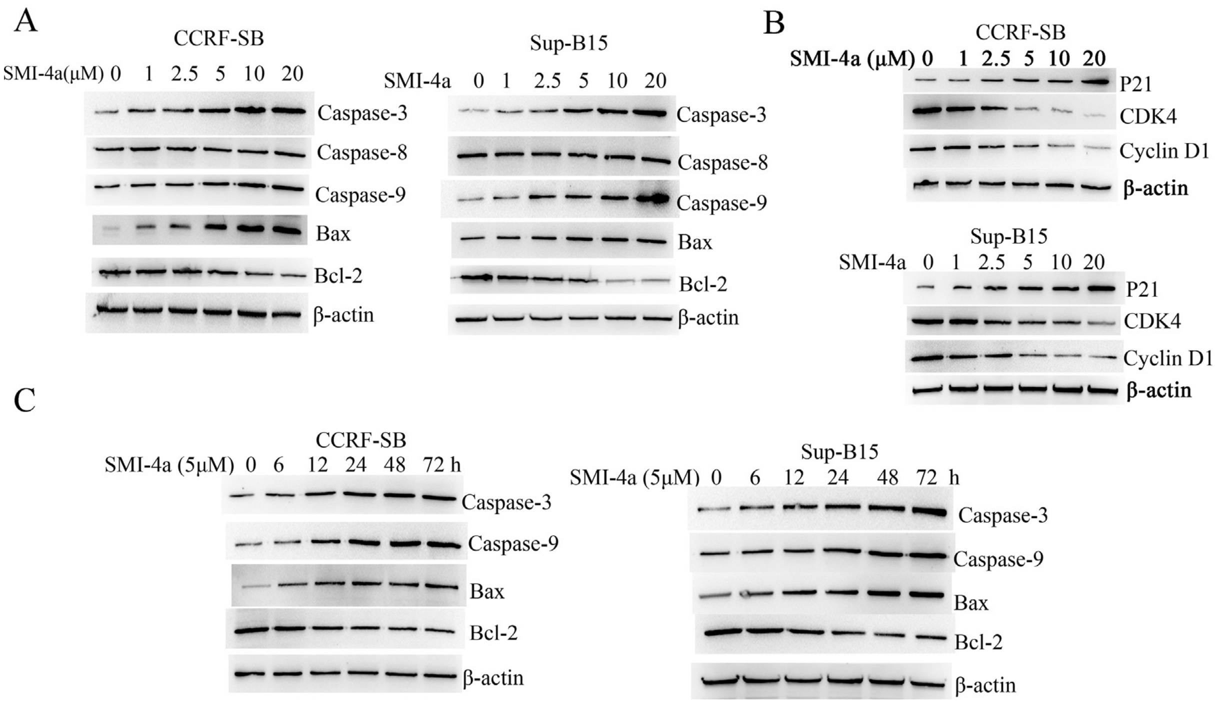

Fig. 4. SMI-4a upregulated the expression of Caspase-3, -8, -9, Bax and P21 proteins in a does-dependent manner. (A) CCRF-SB and Sup-B15 cells were treated with 0, 1, 2.5, 5, 10, and 20 μM SMI-4a for 24 h and the expression levels of Caspase-3, Caspase-8, Caspase-9, Bax and Bcl-2 were detected using Western blot analysis. β-actin was used as a loading control. (B) Sup-B15 and CCRF-SB cells were cultured with different concentrations of SMI-4a for 24 h. The protein levels of P21, CDK4 and Cyclin D1 were detected by Western blot. β-actin was used as loading control. (C) B-ALL cells were treated with 5 μM SMI-4a for 6, 12, 24, 48 and 72 h, after which Western blotting was performed with the β-actin antibody to show equal protein loading.

SMI-4a can modulate the JAK2/STAT3 pathway in B-ALL cells, these cells were treated with SMI-4a and JAK2/STAT3 pathway activation examined. Fig. 5A illustrated that B-ALL cell incubation with SMI-4a induced phosphorylation of JAK2/STAT3 protein in a dose-dependent manner. Meanwhile, SMI-4a treatment was found to decrease HO-1 expression and previous study showed that HO-1 might regulate the JAK2/STAT3 pathway [21,22]. Hence, HO-1 expression was upregulated and inhibited by Hemin (10 μM) and ZnPP (0.05 μM), respectively (Fig. 5B). These treated B-ALL cells were incubated with 5 μM SMI-4a and then JAK2/STAT3 pathway expression analyzed. As a result, Hemin was observed to increase p-JAK2 and p-STAT3 levels, whereas ZnPP decreased levels of these proteins (Fig. 5C). More importantly, after upregulating HO-1 expression with Hemin in B-ALL cells, apoptosis induced by SMI-4a was clearly decreased (Fig. 5D and E). Consistently, when B-ALL cells treated with SMI-4a, upregulating HO-1 increased cell proliferation and downregulating HO-1 decreased cell viability (Fig. 5F). Collectively, the present data demonstrated that SMI-4a induced apoptosis partly through an HO-1-mediated JAK2/STAT3 pathway.

3.5. SMI-4a inhibited B-ALL cell growth and promoted apoptosis in vivo

To observe the effect of SMI-4a on tumor growth in vivo, we placed CCRF-SB cells, which are more sensitive to SMI-4a, subcutaneously in NOD/SCID mice and on day 3 started treatment with this agent. This treatment continued on a twice daily schedule for 5 of 7 days per week until day 21 [15]. As a result, SMI-4a treatment resulted in a significant inhibition on growth of CCR-SB cell-derived tumors (Fig. 6A and B). H&E staining of xenograft tumors showed disorderly and irregular tumor cell arrangement and increased nucleo-cytoplasmic ratio, which is consistent with the pathological characteristics of malignancy (Fig. 6C). Moreover, TUNEL assay revealed the proportion of apoptotic cells was higher in the SMI-4a-treated group (17.56 ± 8.69%) than in the vehicle group (5.46 ± 3.73%, $p < 0.05$, Fig. 6D).

4. Discussion

ALL is the most common childhood cancer, accounting for ~30% of all childhood malignancies, and also occurs in adults. In adults, 75% of cases develop from precursors of B-cell lineage, with the remainder of cases consisting of malignant T-cell precursors [23]. B-ALL is a blood cancer derived from immature B-cell precursors, which usually affects children under 6 years of age [1]. Approximately 20% of patients become resistant to chemotherapy during the treatment of B-ALL [24]. Although > 85% of children with ALL are cured, relapse and/or non-responsive ALL remains a leading cause of cancer-related death in children and young adults [2]. Therefore, the current challenge in B-ALL studies is to seek potential therapeutic targets and novel drugs.

PIMs are serine/threonine kinases that participate in regulating apoptosis, the cell cycle, signal transduction, and transcriptional pathways, which are associated with tumor progression, and chemotherapy resistance [6,7,16,25]. Therefore, serine/threonine PIM protein kinases are promising targets for novel therapy in cancers, and some recent studies have investigated PIM inhibitor effects in various cancers [16,25,26]. In this study, PIM kinase expression in B-ALL was documented using real-time PCR and a higher PIM kinase expression found in B-ALL patients, compared with healthy controls. This study showed that SMI-4a, a small PIM kinase inhibitor, clearly inhibited cell proliferation in B-ALL cell lines CCRF-SB and Sup-B15, indicating that this agent possessed cytotoxicity to these malignant cells. The ability of this agent to regulate cell apoptosis and cell cycle progression was then explored and the results demonstrated that SMI-4a promoted apoptosis and caused cell-cycle arrest in the G_0/G_1 phase, suggesting that SMI-4a attenuated B-ALL cell proliferation by promoting cell apoptosis and blocking cell-cycle progression. In agreement with these results, Lin et al. have found that SMI-4a leads to a G_1-phase cell cycle arrest in pre-T-LBL cells [15]. However, in CML cells, treatment with SMI-4a induced an S-phase cell cycle arrest [16]. These results indicated that SMI-4a might have influenced different cell-cycle phases depending on the

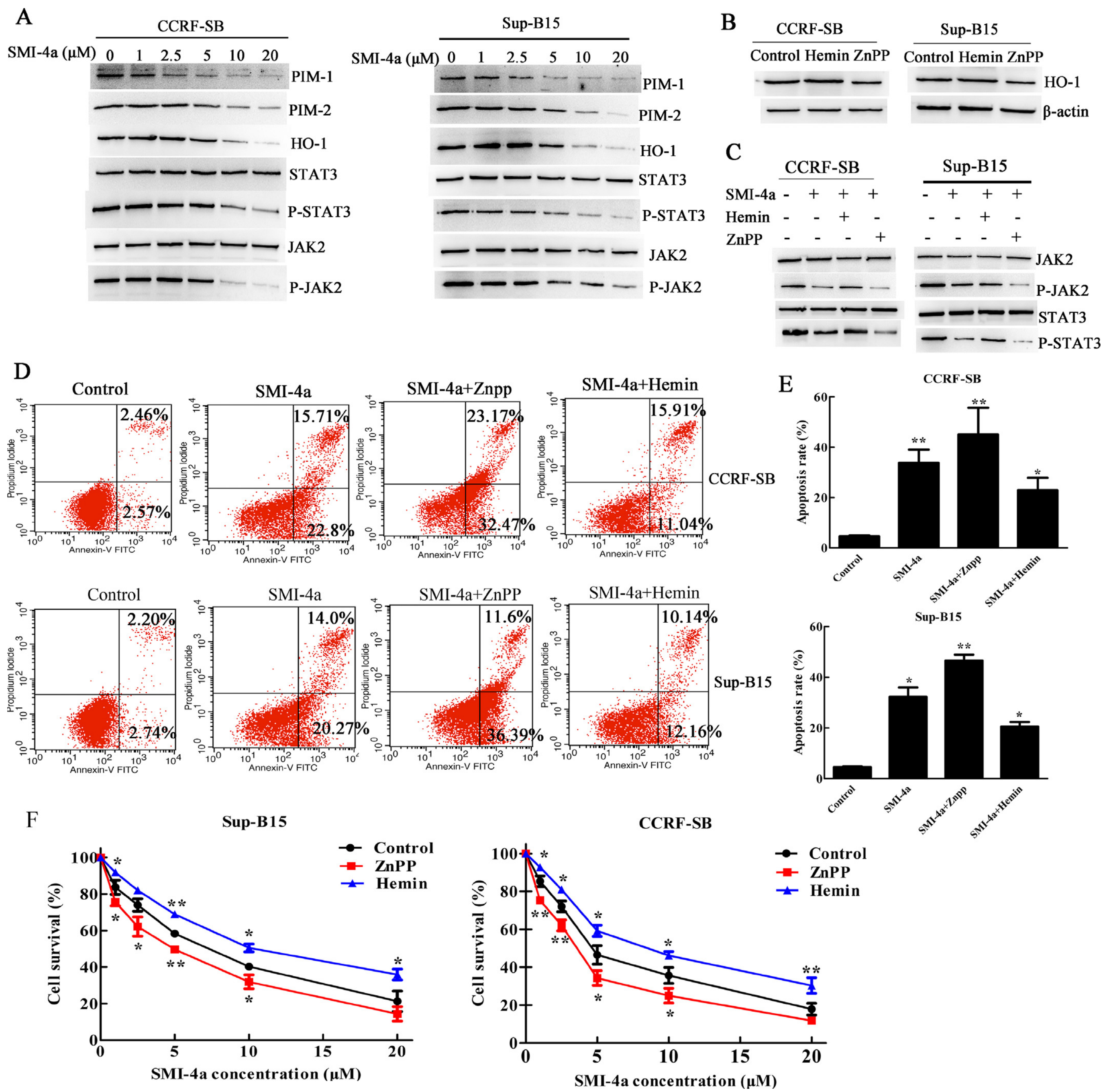

Fig. 5. SMI-4a induced apoptosis partly through HO-1-mediated JAK2/STAT3 pathway. (A) CCRF-SB and Sup-B15 cells were treated with 1, 2.5, 5, 10, and 20 μM SMI-4a for 24 h, after which whole-cell extracts were prepared. Then, Western blot was used to detect PIM-1, PIM-2, HO-1, JAK2, p-JAK2, STAT3 and p-STAT3 expression levels. (B) CCRF-SB and Sup-B15 cells were cultured with 0.05 μM ZnPP or 10 μM Hemin for 24 h, and HO-1 protein level of the treated cells was examined by Western blot. (C) CCRF-SB and Sup-B15 cells were incubated with SMI-4a, Hemin or ZnPP for 24 h, and then analyzed the intracellular levels of p-STAT3 and p-JAK2 using Western blot. The same blots were stripped and reprobed with JAK2 and the STAT3 antibody to verify equal protein loading. (D) Apoptotic rates of CCRF-SB and Sup-B15 cells after HO-1 regulation and SMI-4a treatment were detected by flow cytometry. Data represent one of triplicate tests. (E) Analysis of apoptotic rates of CCRF-SB and Sup-B15 cells in three independent experiments. Data presented as mean ± SD; *, $p < 0.05$ versus DMSO group, and **, $p < 0.01$ versus control group. (F) Sup-B15 and CCRF-SB cells were cultured with different concentration of SMI-4a and ZnPP or Hemin for 24 h and cell viability of these cells was detected by the CCK8 assay. *, $p < 0.05$, **, $p < 0.01$ versus the control.

cellular context and circumstances. The possibility that there were other cell-cycle regulatory factors participating in the process requires further studies.

Our in vitro study showed that SMI-4a could inhibit proliferation and promote apoptosis of B-ALL cells. To investigate the antitumor activity of SMI-4a in vivo, we conducted NOD/SCID mice models in which mice were subcutaneously injected with B-ALL cells. The immunodeficient mouse models, especially those of NOD/SCID mice, are ideal models for in vivo experiments of hematological malignant tumors, as they have a wide range of immunodeficiencies [27]. Currently, subcutaneous injections [15,25,28] are commonly used for the establishment of blood tumors. The results of in vivo study revealed SMI-4a could suppress tumor growth and promote apoptosis in vivo, strengthening the antitumor activity of SMI-4a in B-ALL.

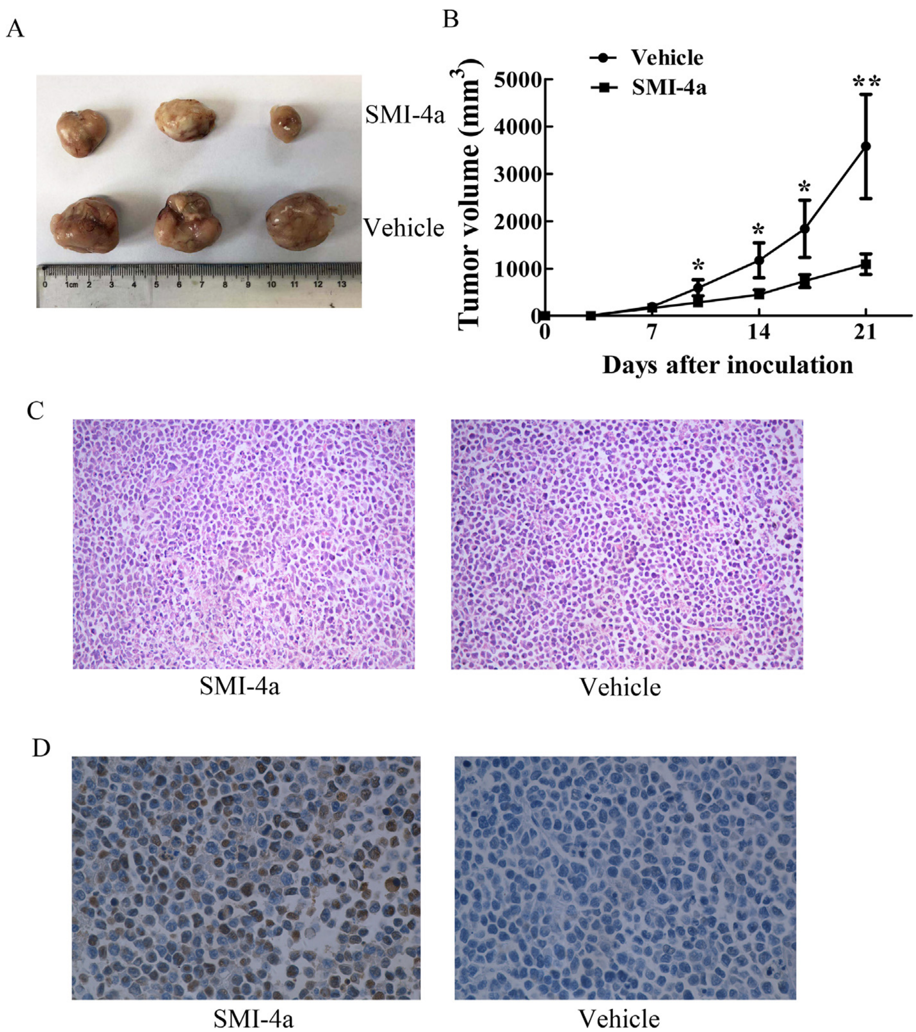

Fig. 6. Effect of SMI-4a on CCRF-SB cell-derived tumor growth in vivo. (A) Photographs of tumors obtained from NOD/SICD mice in respective groups. (B) NOD/SCID mice implanted subcutaneously with CCRF-SB cells were treated twice daily with vehicle or SMI-4a by oral gavage. Tumor size was measured by calipers on day 0, 3, 7, 10, 14, 17, and 21, and calculated as described in "*in vivo* study". Data presented as mean ± SD; *, $p < 0.05$ versus Vehicle group, and **, $p < 0.01$ versus Vehicle group. (C) H&E staining of xenograft tumors in respective groups (×200). (D) Representative images of TUNEL staining (×400). Cells with deep brown nuclei were identified as TUNEL-positive cells.

Prior studies have reported that PIM kinases stimulate cell cycle progression by regulating P21 and p27 proteins [19,29]. Cell cycle progression is precisely controlled by the activity of a series of cyclin dependent kinases (CDKs), which are activated by cyclin binding and negatively regulated by CDK inhibitors [30]. In particular, P21 is one of the most important CDK inhibitors that competitively binds to CDK, resulting in decreased activity of cyclin-CDK complexes and then cell cycle arrest [31]. Under stimulation by various factors, G_1 phase cyclin binds to CDK4 and inactivates pRB by phosphorylation, thus releasing transcription factor E2F and allowing for important transcriptional changes through the G_1/S cell cycle checkpoint [32]. Similarly, here, SMI-4a was found to increase expression of P21 protein. CyclinD1 and CDK4, critical cell-cycle regulators promoting G1/S-phase transition, were found to be downregulated after treatment with SMI-4a. Also, the expressions of Caspase-3, 8, and 9 were evaluated and it was observed that the apoptotic response was activated through either the intrinsic and/or the extrinsic pathway, depending on the origin of the death stimuli. The extrinsic pathway is triggered by tumor necrosis factors and further leads to cleavage and activation of Caspase-8 [33]. The intrinsic pathway is mediated by mitochondria, in response to apoptotic stimuli, as Caspase-9 is activated by apoptosomes, which are complexes formed of cytochrome *c* and apoptotic protease activating factor-1 [34]. Both pathways activate Caspase-3, finally causing PARP cleavage and apoptosis [35]. In the current study, SMI-4a treatment was observed to lead to increased level of Caspase-3 and 9 but had no effect on Caspase-8, indicating that SMI-4a induced apoptosis in B-ALL cells only via the intrinsic mitochondrial pathway. In addition, pro-apoptotic protein Bax expression was observed to be notably upregulated in SMI-4a-treated B-ALL cells. In contrast, Bcl-2 was downregulated in B-ALL cells after incubation with SMI-4a. While it is known that Bcl-2 family proteins are critical regulators of the mitochondrial apoptosis pathway, as a member of the Bcl-2 family, Bcl-2 is an important anti-apoptotic protein. However, Bax is another member of the Bcl-2 family, but it has pro-apoptotic effects [36]. More importantly, an increased Bax/Bcl-2 ratio contributes to activation of Caspase-dependent apoptosis [37]. Based on these findings, we speculated that the upregulation of Bax and downregulation of Bcl-2 caused by SMI-4a resulted in a notable increase in the Bax/Bcl-2 ratio, which further led to upregulation of Caspase-3 and 9 and further induced apoptosis.

HO-1 is a cellular protective enzyme that promotes cell proliferation, inhibits apoptosis, and alleviates inflammation while also increasing drug resistance [38,39]. Both mRNA and protein of HO-1 are constitutively expressed in ALL primary cells and cell lines [40,41], and two HO-1-targeting drugs, PEG-ZnPP and SMA-ZnPP, induce apoptosis and growth arrest in ALL cells [41]. In this study, the effects of HO-1 on apoptosis induced by SMI-4a treatment were determined by incubating B-ALL cells with ZnPP/Hemin and SMI-4a and then assessing the apoptotic rates in these cells. After Hemin was used to upregulate HO-1 expression, the apoptotic rates of B-ALL cells were significantly decreased. In contrast, after B-ALL cells were treated with ZnPP, apoptotic rates increased. These results indicated that SMI-4a affected B-ALL cell apoptosis partly, at least, through HO-1. However, how SMI-4a regulated HO-1 expression remains unknown. Whether SMI-4a directly or indirectly regulates the expression of HO-1, and the relationship between PIMs and HO-1 are still needed to be elucidated in further studies.

A number of cancers depend on JAK2 signaling, including the high-risk subset of B-ALL [42], and constitutive STAT activation is seen in ALL patients and B-ALL cell lines [20,24]. PIM kinase inhibitors have been reported to be associated with the JAK2/STAT3 pathway [14,43], and previous study showed that HO-1 might interfere with the JAK2/STAT3 pathway [21,22]. Interestingly, the present study also found that SMI-4a might have downregulated HO-1 protein expression in B-ALL cells. Based on these findings, a potential effect of HO-1 was proposed here regarding the regulation of SMI-4a-induced activation of the JAK2/STAT3 pathway. As expected, Western blot showed down-regulation of p-JAK2 and p-STAT3 after SMI-4a treatment, whereas Hemin-treated B-ALL cells had increased p-JAK2 and p-STAT3 expression. Based on these findings, a potential mechanism was proposed here that was behind the observed inhibitory effects of SMI-4a in B-ALL cells. In short, SMI-4a downregulated the expression of HO-1 and inhibited the activation of the JAK2/STAT3 pathway, promoting B-ALL cell apoptosis and inhibiting cell proliferation.

In conclusion, the present results pointed to an overexpression of PIMs in B-ALL patients. The PIM inhibitor SMI-4a clearly repressed B-ALL cell growth via apoptosis induction and G_0/G_1-phase cycle arrest. SMI-4a downregulated PIMs and led to low HO-1 expression as well. Upregulation of HO-1 inhibited the apoptosis of B-ALL cells induced by SMI-4a. Therefore, SMI-4a presented the potential for a novel therapeutic strategy in B-ALL treatment, and the combined effect of SMI-4a and other common chemotherapy drugs in B-ALL should be further explored.

Conflict of interest

The authors declare no conflict of interest.

Acknowledgements

This study was supported by the National Natural Science Foundation of China (No. 81670006, NO. 81660616).

References

[1] S. Loghavi, J.L. Kutok, J.L. Jorgensen, B-acute lymphoblastic leukemia/lymphoblastic lymphoma, Am. J. Clin. Pathol. 144 (3) (2015) 393–410.
[2] S. Thota, A. Advani, Inotuzumab ozogamicin in relapsed B-cell acute lymphoblastic leukemia, Eur. J. Haematol. 98 (5) (2017) 425–434.
[3] J. Xu, et al., PIM-1 contributes to the malignancy of pancreatic cancer and displays diagnostic and prognostic value, J. Exp. Clin. Cancer Res. 35 (1) (2016).
[4] J. Asano, et al., The serine/threonine kinase Pim-2 is a novel anti-apoptotic mediator in myeloma cells, Leukemia 25 (7) (2011) 1182–1188.
[5] Y.-Y. Li, et al., Pim-3, a proto-oncogene with serine/threonine kinase activity, is aberrantly expressed in human pancreatic cancer and phosphorylates bad to block bad-mediated apoptosis in human pancreatic cancer cell lines, Cancer Res. 66 (13) (2006) 6741–6747.
[6] S. Decker, et al., PIM kinases are essential for chronic lymphocytic leukemia cell survival (PIM2/3) and CXCR4-mediated microenvironmental interactions (PIM1), Mol. Cancer Ther. 13 (5) (2014) 1231–1245.
[7] J. Chen, et al., Pim-1 plays a pivotal role in hypoxia-induced chemoresistance, Oncogene 28 (28) (2009) 2581–2592.
[8] K.T. Kim, Pim-1 is up-regulated by constitutively activated FLT3 and plays a role in FLT3-mediated cell survival, Blood 105 (4) (2005) 1759–1767.
[9] K. Meja, et al., PIM and AKT kinase inhibitors show synergistic cytotoxicity in acute myeloid leukaemia that is associated with convergence on mTOR and MCL1 pathways, Br. J. Haematol. 167 (1) (2014) 69–79.
[10] J. Lu, et al., Pim2 is required for maintaining multiple myeloma cell growth through modulating TSC2 phosphorylation, Blood 122 (9) (2013) 1610–1620.
[11] S. Kreuz, et al., Loss of PIM2 enhances the anti-proliferative effect of the pan-PIM kinase inhibitor AZD1208 in non-Hodgkin lymphomas, Mol. Cancer 14 (1) (2015) 205.
[12] K. Kapelko-Słowik, et al., Expression of PIM-2 and NF-κB genes is increased in patients with acute myeloid leukemia (AML) and acute lymphoblastic leukemia (ALL) and is associated with complete remission rate and overall survival, Postepy Hig. Med. Dosw. (Online) 67 (2013) 553–559.
[13] M. Bellon, L. Lu, C. Nicot, Constitutive activation of Pim1 kinase is a therapeutic target for adult T-cell leukemia, Blood 127 (20) (2016) 2439–2450.
[14] M. Szydłowski, et al., Expression of PIM kinases in Reed-Sternberg cells fosters immune privilege and tumor cell survival in Hodgkin lymphoma, Blood 130 (12) (2017) 1418–1429.
[15] Y.W. Lin, et al., A small molecule inhibitor of Pim protein kinases blocks the growth of precursor T-cell lymphoblastic leukemia/lymphoma, Blood 115 (4) (2009) 824–833.
[16] R.-F. Fan, et al., PIM-1 kinase inhibitor SMI-4a exerts antitumor effects in chronic myeloid leukemia cells by enhancing the activity of glycogen synthase kinase 3β, Mol. Med. Rep. 16 (4) (2017) 4603–4612.
[17] X. Kuang, et al., miR-378 inhibits cell growth and enhances apoptosis in human myelodysplastic syndromes, Int. J. Oncol. 49 (5) (2016) 1921–1930.
[18] N. Keane, et al., Targeting the Pim kinases in multiple myeloma, Blood Cancer J. 5 (2015) e325.
[19] L. Chen, et al., Mechanisms of cytotoxicity to Pim kinase inhibitor, SGI-1776, in acute myeloid leukemia, Blood 118 (3) (2011) 693–702.
[20] T. Lin, S. Mahajan, D. Frank, STAT signaling in the pathogenesis and treatment of leukemias, Oncogene 19 (21) (2000) 2496–2504.
[21] S. Tang, et al., Histone deacetylase inhibitor BG45-mediated HO-1 expression induces apoptosis of multiple myeloma cells by the JAK2/STAT3 pathway, Anti-Cancer Drugs 29 (1) (2018) 61–74.
[22] B. Elguero, et al., Unveiling the association of STAT3 and HO-1 in prostate cancer: role beyond heme degradation, Neoplasia 14 (11) (2012) 1043–1056.
[23] T. Terwilliger, M. Abdul-Hay, Acute lymphoblastic leukemia: a comprehensive review and 2017 update, Blood Cancer J. 7 (6) (2017) e577.
[24] S.-S. Han, S. Han, N.L. Kamberos, Piperlongumine inhibits the proliferation and survival of B-cell acute lymphoblastic leukemia cell lines irrespective of glucocorticoid resistance, Biochem. Biophys. Res. Commun. 452 (3) (2014) 669–675.
[25] E. Keeton, et al., AZD1208, a potent and selective pan-Pim kinase inhibitor, demonstrates efficacy in preclinical models of acute myeloid leukemia, Blood 123 (6) (2014) 905–913.
[26] A.V. Moorman, New and emerging prognostic and predictive genetic biomarkers in B-cell precursor acute lymphoblastic leukemia, Haematologica 101 (4) (2016) 407–416.
[27] Mouse Models for Drug Discovery. Methods and Protocols, Second edition, Anticancer Res 36(8) (2016), p. 4371.
[28] J. Cui, et al., MicroRNA143 increases cell apoptosis in myelodysplastic syndrome through the Fas/FasL pathway both in vitro and in vivo, Int. J. Oncol. 53 (5) (2018) 2191–2199.
[29] Y. Zhang, Z. Wang, N. Magnuson, Pim-1 kinase-dependent phosphorylation of p21Cip1/WAF1 regulates its stability and cellular localization in H1299 cells, Mol. Cancer Res. 5 (9) (2007) 909–922.
[30] X. Graña, E. Reddy, Cell cycle control in mammalian cells: role of cyclins, cyclin dependent kinases (CDKs), growth suppressor genes and cyclin-dependent kinase inhibitors (CKIs), Oncogene 11 (2) (1995) 211–219.
[31] J. Harper, et al., The p21 Cdk-interacting protein Cip1 is a potent inhibitor of G1 cyclin-dependent kinases, Cell 75 (4) (1993) 805–816.
[32] L. Bockstaele, et al., Regulation of CDK4, Cell Div 1 (2006) 25.
[33] D. Wallach, et al., Tumor necrosis factor receptor and Fas signaling mechanisms, Annu. Rev. Immunol. 17 (1999) 331–367.
[34] P. Li, et al., Cytochrome c and dATP-dependent formation of Apaf-1/caspase-9 complex initiates an apoptotic protease cascade, Cell 91 (4) (1997) 479–489.
[35] S. Goldar, et al., Molecular mechanisms of apoptosis and roles in cancer development and treatment, Asian Pac. J. Cancer Prev. 16 (6) (2015) 2129–2144.
[36] W. Eldehna, et al., Design, synthesis and in vitro antitumor activity of novel N-substituted-4-phenyl/benzylphthalazin-1-ones, Eur. J. Med. Chem. 89 (2015) 549–560.
[37] A. Czerwonka, et al., Anticancer effect of the water extract of a commercial Spirulina (Arthrospira platensis) product on the human lung cancer A549 cell line, Biomed. Pharmacother. 106 (2018) 292–302.
[38] W. Wu, et al., Potential crosstalk of the interleukin-6-heme oxygenase-1-dependent mechanism involved in resistance to lenalidomide in multiple myeloma cells, FEBS J. 283 (5) (2016) 834–849.
[39] D. Ma, et al., Crucial role of heme oxygenase-1 in the sensitivity of acute myeloid leukemia cell line Kasumi-1 to ursolic acid, Anti-Cancer Drugs 25 (4) (2014) 406–414.
[40] Y. Guo, et al., Up-regulation of HO-1 promotes resistance of B-cell acute lymphocytic leukemia cells to HDAC4/5 inhibitor LMK-235 via the Smad7 pathway, Life Sci. 207 (2018) 386–394.
[41] S. Cerny-Reiterer, et al., Identification of heat shock protein 32 (Hsp32) as a novel target in acute lymphoblastic leukemia, Oncotarget 5 (5) (2014) 1198–1211.
[42] S. Wu, et al., Activity of the type II JAK2 inhibitor CHZ868 in B cell acute lymphoblastic leukemia, Cancer Cell 28 (1) (2015) 29–41.
[43] T. Shirogane, et al., Synergistic roles for Pim-1 and c-Myc in STAT3-mediated cell cycle progression and antiapoptosis, Immunity 11 (6) (1999) 709–719.